Performance of Computational Fluid Dynamics and Finite Element Methods for Modeling Downslope Displacement of Failed Soil from Submarine Landslides

Binoy Debnath & Bipul Hawlader
Memorial University, St. John's, Newfoundland and Labrador, Canada
Sujan Dutta
Royal Military College of Canada, Kingston, Ontario, Canada
Tarun Sheel
Memorial University, St. John's, Newfoundland and Labrador, Canada

ABSTRACT
Submarine landslides are considered one of the major geohazards in offshore oil and gas development activities. After the failure of a slope, the failed soil mass may travel over a large distance during which it disintegrates into smaller pieces and is fluidized due to interaction with surrounding water. For modeling submarine landslides and their impact on offshore structures, two approaches are commonly used: geotechnical and fluid mechanics approaches. Comparison between these two approaches for modelling run-out of a failed soil mass is presented in this paper. Large deformation finite-element analyses are performed using the Coupled Eulerian–Lagrangian (CEL) approach in Abaqus FE software. The computational fluid dynamics approach in ANSYS CFX is used to model the same process where the shear resistance of soft clay sediment is defined as a non-Newtonian using dynamic viscosity. The similarities and differences between the simulation results using these two approaches are discussed.

RÉSUMÉ
Les glissements de terrain sous-marins sont considérés comme l'un des géorisques majeurs dans les activités de développement pétrolier et gazier offshore. Après la rupture d'une pente, la masse de sol défaillante peut se déplacer sur une grande distance au cours de laquelle elle se désintègre en plus petits morceaux et est fluidisée en raison de l'interaction avec l'eau environnante. Pour la modélisation des glissements de terrain sous-marins et leur impact sur les structures offshore, deux approches sont couramment utilisées: les approches géotechniques et la mécanique des fluides. La comparaison de ces deux approches pour la modélisation à partir d'une masse de sol défaillante est présentée dans cet article. Les analyses par éléments finis de grandes déformations sont réalisées en utilisant l'approche Coupled Eulerian-Lagrangian (CEL) dans le logiciel Abaqus FE. L'approche de la dynamique des fluides computationnelle dans ANSYS CFX est utilisée pour modéliser le même processus où la résistance au cisaillement des sédiments d'argile molle est définie comme une viscosité dynamique non-newtonienne. Les similitudes et les différences entre les résultats de simulation utilisant ces deux approches sont discutées.

1 INTRODUCTION

Many small to large-scale landslides occur in offshore environments. After a submarine landslide, the failed soil mass or debris could travel hundreds of kilometers and impact offshore infrastructures in the downslope areas, such as deep water as-laid suspended pipelines. In some cases it travels at a very high speed, typically in the range of 7–30 m/s or higher, as noted by De Blasio et al. (2004a) and Sahdi et al. (2014). The run-out distance and the velocity of the failed soil are important in the design of offshore structures and to evaluate potential risks associated with submarine landslides.

After the failure of a slope, the failed soil mass is transferred into different phases during the process of run-out due to the effects of various factors, including the change in shear strength, remoulding and fluidization. In the initial stages, the failed sediment blocks carry the parent soil property and do not experience significant loss of shear strength. These blocks are generally called a "glide block" and "out-runner block." However, after travelling a large distance, the cohesive sediment transfers to a slurry of high clay concentration and is called as "debris flow" and "turbidity current."

Two approaches are commonly used to model submarine landslides and their impact. In the geotechnical approach, the soil is modeled using the undrained shear strength. As the failed soil mass travels a large distance, large deformation finite-element modeling techniques are used to simulate this process. For example, Dey et al. (2016) used the Coupled Eulerian–Lagrangian (CEL) approach in Abaqus FE software to model the failure initiated through a thin weak layer and subsequent propagation in the upper clay layers. The large deformation finite-element (LDFE) approach based on "remeshing and interpolation technique by small strain (RITSS)" has been used by other researchers (Zhu and Randolph 2010; Liu et al. 2011; Wang et al. 2013). Other approaches, such as material point methods, have also been used in some studies to simulate the run-out process (Ma 2015; Dong et al. 2017).

In the fluid mechanics approach, the debris is typically modeled as non-Newtonian viscous fluids where the shear resistance is defined using the dynamic viscosity of the fluid (soft clay or clay slurry), as a function of shear strain rate. Imran et al. (2001) conducted numerical modelling by developing the finite-difference program BING to simulate the debris flow using the Herschel–Bulkley and a bilinear rheology for viscoplastic fluid. This program and its modified form have been used by a number of researchers for modeling debris flow (Marr et al. 2002; De Blasio et al. 2003, 2004a, 2004b, 2005; Locat et al. 2004; Elverhøi et al. 2010). The BING code developed by Imran et al. (2001) is based on constant dynamic viscosity as well as constant yield strength. De Blasio et al. (2003) developed an approach to model the decrease in shear stress due to shear wetting. Gauer et al. (2005) showed that a computational fluid dynamics approach could be used to simulate the initiation and progressive failure of large-scale submarine landslides.

The aim of this research program is to develop appropriate numerical modeling tools to simulate the initiation and run-out of submarine landslides. A comparison of run-out simulations using a large deformation finite element program and a computational fluid dynamics approach is presented in this paper.

2 NUMERICAL MODELING TOOLS

The following two numerical approaches are used to model large deformation of the failed soil mass.

2.1 Finite-element analysis

The coupled Eulerian–Lagrangian (CEL) approach available in Abaqus Version 6.14.2 FE software is used for FE analyses. The soil is modeled as an Eulerian material to simulate large deformation of the failed soil. Note that, unlike the approaches used for modeling Eulerian materials in typical computational fluid dynamics (CFD) programs, as the one discussed in the following section, the Eulerian time integration in Abaqus FE program is performed in the computational solid mechanics framework. The fundamental concept of CEL analysis, benchmark studies and its applications to large-scale landslide modeling could be found in previous studies (Benson and Okazawa 2004; Dutta and Hawlader 2016; Dey et al. 2016). Unlike typical Lagrangian FE formulations, where the material time derivatives are used, the Eulerian formulation is based on spatial time derivatives. Abaqus CEL uses operator splitting to solve the governing equations. Each time step has two phases of calculations: a conventional Lagrangian phase followed by an Eulerian phase. In the Eulerian phase, the solution obtained from the Lagrangian phase is mapped back to the spatially fixed Eulerian mesh.

2.2 Computational fluid dynamics analysis

The computational fluid dynamics (CFD) approach available in ANSYS CFX Version 16.2 is used to model run-out of the failed soil mass. Unlike Abaqus CEL, a finite-volume technique is used in CFX for modeling Eulerian material flow. The momentum and mass transfer processes are modelled using the Navier–Stokes equations, which has been developed applying Newton's second law of motion to fluid elements (soft clay sediment in the present study).

Both of these numerical tools allow only three-dimensional modeling. In addition, in both cases, Eulerian materials flow through the fixed mesh and therefore numerical issues related to mesh distortion are not encountered. Note that mesh distortion is one of the main limitations of typical Lagrangian-based FE programs and therefore cannot be used for this type of large-deformation run-out modeling.

3 PROBLEM STATEMENT

A hypothetical clay block of trapezoidal shape on a mild inclined seabed, having slope angle (β) of 5°, as shown in Figure 1, is modeled. In an offshore environments, the failed soil mass might accumulate due to a submarine landslide in the downslope areas when the propagation of failure is arrested by strong soil or reduction in slope angle (Trapper et al. 2015; Dey et al. 2016). In a favourable condition—higher downslope angle and sufficient height of the accumulated soil—this clay block could travel over the seabed and impact offshore facilities.

Although the shape of the accumulated soil on the seabed that results from submarine landslides varies widely, as observed in post-slide investigation (Prior et al. 1982; Van Weering et al. 1998) and numerical simulations (Trapper et al. 2015; Dey et al. 2016), a trapezoidal shape of soil block is assumed in this study for simplicity to show the performance of these two numerical approaches for modeling run-out (Fig. 1).

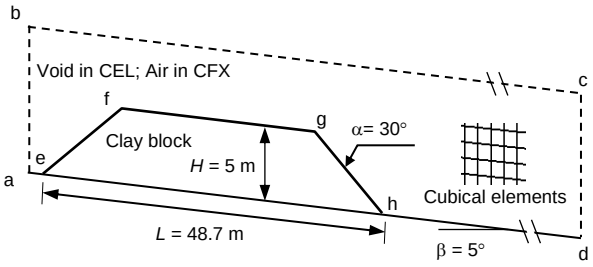

Figure 1. Problem statement

4 MODEL SETUP

4.1 CEL model setup

As the CEL allows only three-dimensional modeling, in order to simulate the plane strain condition, FE analysis is performed with only one element length in the out-of-plane direction. Eight-node Eulerian brick elements (EC3D8R in Abaqus) of 0.25-m length is used to discretize the domain, except for the mesh sensitivity analyses. The FE domain

has three parts: (i) a clay block (e.g. 'efgh' in Fig. 1 for the initial condition); (ii) a void space outside the soil block (abcdhgfe) to accommodate the displace soil; and (iii) a rigid Lagrangian body below the line 'ad' in Fig. 1.

The initial condition is defined using the Eulerian Volume Fraction (EVF) available in Abaqus CEL. For an element, EVF = 1 means that the element is filled with soil and EVF = 0 means the element is void. A fractional value of EVF means that the element is partially filled with soil. The density of submerged soil is assigned to all the soil elements.

Zero velocity boundary conditions are applied normal to all the vertical faces of domain shown in Fig. 1. No boundary conditions are applied along the clay–void interface, which allows the displacement of clay in the void space when needed. Rough condition is used to define the interface behaviour between clay and rigid body.

FE analysis consists of two loading steps. Firstly, in the gravitational step, the gravitational acceleration is applied quickly to create geostatic stresses in the soil elements while maintaining the ratio between horizontal and vertical stresses equal to 1.0. In the next step, no external load is applied and the analysis is continued over a period of time until the instantaneous velocity of the soil elements becomes negligible.

4.2 CFX model setup

Similar to CEL, the three-dimensional CFX model is developed with one element length in the out-of-plane direction, in order to simulate the plane strain condition. The domain is discretized into cubical elements of 0.25 m length. A submerged unit weight of 5.9 kN/m^3 is assigned to the clay elements.

Two types of materials are considered: soft clay in the clay block (efgh) and air outside the block. Both clay and air are modeled as homogeneous multiphase Eulerian materials.

A symmetry plane boundary condition is applied to the vertical faces. The interface behaviour between bottom boundary and clay is defined using a no-slip boundary condition.

5 MODELING OF SOIL

Deepwater offshore sediments are typically soft clays. The behaviour of soft clay sediment is modeled using a uniform undrained shear strength (s_u) of 2.1 kPa. In Abaqus CEL, it is defined using the yield strength (= $2s_u$), adopting the von Mises yield criterion in total stress analysis.

In CFX, there is no direct option to define the undrained shear strength of clay. Therefore, it is defined using the dynamic viscosity of non-Newtonian fluid (μ_d), which is related to s_u as $s_u/\dot{\gamma}$, where $\dot{\gamma}$ is the shear strain rate. Further details on implementation of soft clay sediment behaviour in CFX are available in Dutta and Hawlader (2018). The built-in dynamic viscosity of air of 1.831×10^{-5} Pa.s in CFX is used, which does not have significant effects on run-out. Table 1 shows the geometry and geotechnical parameters used in numerical analyses. These parameters have been selected from a review of geotechnical properties of offshore clay sediments reported in the literature (Kvalstad et al. 2005; Wang et al. 2013).

Table 1. Geometry and soil parameters used in analysis

Parameter	Value
Initial base length of clay block, L (m)	48.7
Initial height of clay block, H (m)	5.0
Side slope of clay block, α (°)	30
Seabed slope angle, β (°)	5
Submerged unit weight of clay, γ' (kN/m^3)	5.9
Undrained shear strength of clay, s_u (kPa)	2.1
Undrained Young's modulus, E_u (kPa)*	$500s_u$
Undrained Poisson's ratio, ν_u*	0.495

*E_u and ν_u are needed only for CEL analysis

6 RESULTS

In the assessment of geohazard risks associated with submarine landslides two key parameters need to be considered: (i) run-out distance and (ii) velocity of the failed soil mass. The former item provides information on whether a submarine landslide could impact an offshore structure in the downslope area. If a structure is located in the run-out zone, the drag force resulting from the failed soil mass depends on impact velocity (Zakeri and Hawlader 2013; Dutta and Hawlader 2018).

6.1 Frontal velocity and run-out distance

Figure 2 shows the calculated run-out distances using CFX and CEL. In both analyses, the Eulerian material (soil) flows through the fixed mesh. Therefore, the deformed positon of the soil block cannot be obtained directly from nodal displacements, as in typical Lagrangian-based FE analysis. Based on simulation results, the coordinates of the front of the failed soil mass with time is obtained, and the horizontal distance from the initial positon of the clay block is calculated to obtain the run-out distance. The solid line in Fig. 2(a) for 0.25-m mesh shows that the frontal velocity starts to increase immediately after the start of calculation because of plastic deformation and failure of slope in the downslope side (right side of the clay block in Fig. 1). The maximum frontal velocity of ~ 4 m/s is calculated at t ~ 3 s. Thereafter, the velocity decreases and, at t ~ 10 s, the velocity becomes almost zero. In other words, the downslope movement of the failed soil mass stops at this time.

The solid line in Fig. 2(a) also shows that the runout distance increases with time and, at t ~ 10 s, the maximum runout of ~ 18 m is obtained. At this time, the soil mass spreads horizontally over a large distance of ~ 68 m (originally 48.7 m), which increases the shear resistance at the bottom of the failed soil mass. Moreover, as it spreads over a large distance, the height of the soil mass reduces. Therefore, the downslope movement of the soil block stops.

Figure 2(b) shows a similar calculation using Abaqus CEL. This analysis also shows that the velocity increases with time for $t \leq 3$ s and then reduces to zero at $t \sim 10$ s. A comparison between the results obtained from these two methods shows that both numerical techniques can simulate large deformation of the failed soil mass.

6.2 Velocity of soil elements

In addition to frontal velocity, as presented in Fig. 2, the velocity of soil elements during the process of run-out is also compared. Figure 3(a) shows that, at $t \sim 2.8$ s, a maximum velocity of ~ 4 m/s occurs in a small zone near the front of the failed soil mass. The magnitude of velocity gradually decreases with distance. In the upslope side (left side of the clay block in Fig. 1), the velocity is almost zero, which indicates that this side of the soil block does not fail. Figure 3(d) shows a similar instantaneous velocity contour obtained from Abaqus CEL. At $t = 6$ s, the velocity of the soil elements reduces as compared to those at $t = 2.8$ s (Figs. 3(b) & 3(e)). Finally, at $t = 9$ s, the velocity is very small, indicating the completion of run-out.

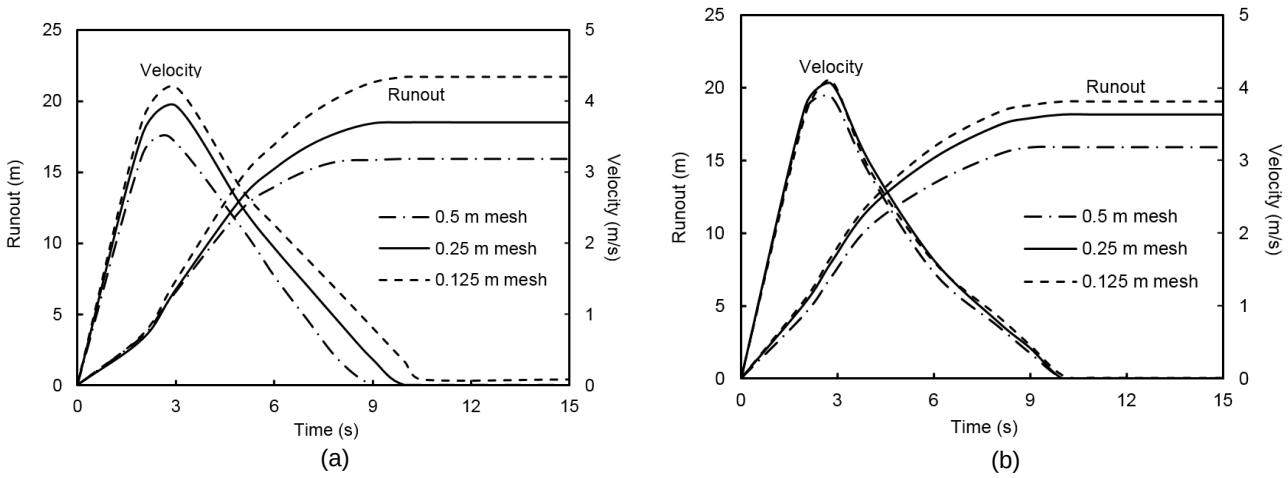

Figure 2. Frontal velocity and runout: (a) using CFX, (b) using CEL

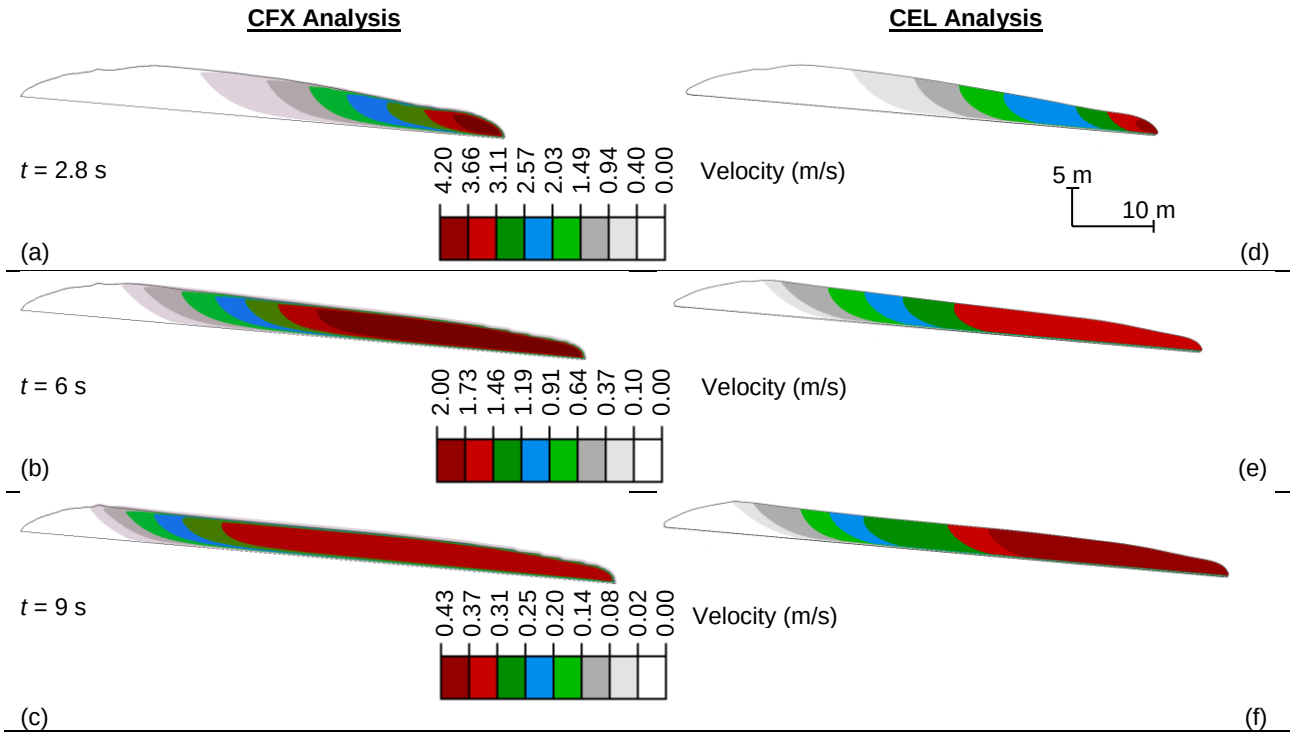

Figure 3. Comparison of soil element velocities in CFX and CEL analysis

6.3 Mesh sensitivity

Analyses are also performed for two more mesh sizes (cubical elements of 0.125 m and 0.5 m). Figure 2(a) shows that velocity and run-out distance increase with a decrease in mesh size. This is because of failure of soil through a thinner zone in a finer mesh. A mesh sensitivity analysis is also performed with Abaqus CEL for similar mesh sizes. Compared to CFX, frontal velocity and run-out distance are less sensitive to mesh size in Abaqus CEL for the mesh sizes considered. This difference might result from differences in solution techniques used in these two computational tools. Note that mesh sensitivity has also been observed in run-out simulations with the material point method (Dong et al. 2017). Further studies are required to resolve this issue.

7 CONCLUSIONS

Run-out of failed soil mass resulting from a submarine landslide could pose a significant threat to offshore structures. Numerical simulation of run-out of a failed soil mass is simulated using a large-deformation finite-element modeling technique and a computational fluid dynamics approach. Comparison of simulation results for the present idealized condition shows similar results. The present study shows some preliminary simulation results. A number of factors, such as strain-softening of clay sediments, strain rate effects on undrained shear strength, possible water entrainment under the soil block during downslope movement that could cause hydroplaning, need to be further investigated.

8 ACKNOWLEDGEMENTS

The work presented in this paper has been funded by the Natural Sciences and Engineering Research Council of Canada (NSERC), Mitacs and Statoil Canada.

9 REFERENCES

Benson, D.J. and Okazawa, S. 2004. Contact in a multi-material Eulerian finite element formulation, *Computer Methods in Applied Mechanics and Engineering*, 193(39–41 SPEC. ISS.): 4277–4298.

De Blasio, F.V., Issler, D., Elverhøi, A., Harbitz, C.B., Ilstad, T., Bryn, P., Lien, R. and Løvholt, F. 2003. Dynamics, velocity and run-out of the giant Storegga slide, *In Submarine Mass Movements and Their Consequences*, Springer, pp. 223–230.

De Blasio, F.V., Engvik, L., Harbitz, C.B. and Elverhøi, A. 2004a. Hydroplaning and submarine debris flows, *Journal of Geophysical Research*, 109(C1): C01002.

De Blasio, F.V., Elverhøi, A., Issler, D., Harbitz, C.B., Bryn, P. and Lien, R. 2004b. Flow models of natural debris flows originating from overconsolidated clay materials, *Marine Geology*, 213: 439–455.

De Blasio, F.V., Elverhøi, A., Issler, D., Harbitz, C.B., Bryn, P. and Lien, R. 2005. On the dynamics of subaqueous clay rich gravity mass flows - The giant Storegga slide, Norway, *Marine and Petroleum Geology*, 22: 179–186.

Dey, R., Hawlader, B.C., Phillips, R. and Soga, K. 2016. Numerical modelling of submarine landslides with sensitive clay layers, *Géotechnique*, 66(6): 454–468.

Dong, Y., Wang, D. and Randolph, M.F. 2017. Runout of submarine landslide simulated with material point method, *Journal of Hydrodynamics*, 29(3): 438–444.

Dutta, S. and Hawlader, B. 2016. A comparative study of advanced numerical methods for large deformation problems using cylindrical object penetration into seabed, *69th Canadian Geotechnical Conference, GeoVancouver 2016*, 2–5 October, Vancouver, British Columbia, Canada.

Dutta, S. and Hawlader, B. 2018. Pipeline–soil–water interaction modeling for submarine landslide impact on suspended offshore pipelines, *Géotechnique* (accepted).

Elverhøi, A., Breien, H., De Blasio, F.V., Harbitz, C.B. and Pagliardi, M. 2010. Submarine landslides and the importance of the initial sediment composition for run-out length and final deposit, *Ocean Dynamics*, 60(4): 1027–1046.

Gauer, P., Kvalstad, T.J., Forsberg, C.F., Bryn, P. and Berg, K. 2005. The last phase of the Storegga Slide: Simulation of retrogressive slide dynamics and comparison with slide-scar morphology, *Marine and Petroleum Geology*, 22: 171–178.

Imran, B.J., Member, A., Parker, G., Locat, J. and Lee, H. 2001. 1D numerical model of muddy subaqueous and subaerial debris flows, *Journal of Hydraulic Engineering*,127: 959–968.

Kvalstad, T.J., Nadim, F., Kaynia, A.M., Mokkelbost, K.H. and Bryn, P. 2005. Soil conditions and slope stability in the Ormen Lange area, *Marine Petroleum Geology*, 22: 299–310.

Liu, J., Yu, L., Kong, X. and Hu, Y., 2011. Large displacement finite element analysis of submarine slide due to gas hydrate dissociation, *International Conference on Ocean, Offshore and Arctic Engineering*, ASME, June 19–24, Rotterdam, Netherlands, pp. 861–865.

Locat, J., Lee, H.J., Locat, P. and Imran, J. 2004. Numerical analysis of the mobility of the Palos Verdes debris avalanche, California, and its implication for the generation of tsunamis, *Marine Geology*, 203: 269–280.

Ma, J. 2015. Numerical modelling of submarine landslides and their impact to underwater infrastructure using the material point method, PhD thesis, the University of Western Australia.

Marr, J.G., Elverhøi, A., Harbitz, C.B., Imran, J. and Harff, P. 2002. Numerical simulation of mud-rich subaqueous debris flows on the glacially active margins of the Svalbard-Barents Sea, *Marine Geology*, 188: 351–364.

Prior, D.B., Bornhold, B.D., Coleman, J.M. and Bryant, W.R. 1982. Morphology of a submarine slide, Kitimat Arm, British Columbia, *Geology*, 10(11): 588–592.

Sahdi, F., Gaudin, C., White, D.J., Boylan, N. and Randolph, M.F. 2014. Centrifuge modelling of active slide - pipeline loading in soft clay, *Géotechnique*, 64(1): 213–226.

Trapper, P.A., Puzrin, A.M. and Germanovich, L.N. 2015.

Effects of shear band propagation on early waves generated by initial breakoff of tsunamigenic landslides, *Marine Geology*, 370: 99–112.

Van Weering, T.C.E., Nielsen, T., Kenyon, N.H., Akentieva, K. and Kuijpers, A.H. 1998. Large submarine slides on the NE Faeroe continental margin, *Geological Processes on Continental Margins: Sedimentation, Mass-Wasting and Stability*, 129(1): 5–17.

Wang, D., Randolph, M.F. and White, D.J. 2013. A dynamic large deformation finite element method based on mesh regeneration, *Computers and Geotechnics*, 54: 192–201.

Zakeri, A. and Hawlader, B. 2013. Drag forces caused by submarine glide block or out-runner block impact on suspended (free-span) pipelines—numerical analysis, *Ocean Engineering*, 67: 89–99.

Zhu, H. and Randolph, M.F. 2010. Large deformation finite-element analysis of submarine landslide interaction with embedded pipelines, *International Journal of Geomechanics*, ASCE, 10(4): 145–152.